

Single-photon storing in coupled non-Markovian atom-cavity system

H. Z. Shen, M. Qin, and X. X. Yi

School of Physics and Optoelectronic Technology, Dalian University of Technology, Dalian 116024, China

(Received 24 June 2013; published 20 September 2013)

Taking the non-Markovian effect into account, we study how to store a single photon of arbitrary temporal shape in a single atom coupled to an optical cavity. Our model applies to Raman transitions in three-level atoms, with one branch of the transition controlled by a driving pulse, and the other coupled to the cavity. For any couplings of input field to the optical cavity and detunings of the atom from the driving pulse and cavity, we extend the input-output relation from Markovian to non-Markovian dynamics. For most possible photon shapes, we derive an analytic expression for the driving pulse in order to completely map the input photon into the atom. We find that the amplitude of the driving pulse depends only on the detuning of the atom from the frequency of the cavity, i.e., the detuning of the atom to the driving pulse has no effect on the strength of the driving pulse.

DOI: [10.1103/PhysRevA.88.033835](https://doi.org/10.1103/PhysRevA.88.033835)

PACS number(s): 42.50.Pq, 32.80.Qk, 03.67.Lx

I. INTRODUCTION

Quantum networks composed of local nodes and quantum channels have attracted much attention in recent years due to a wide range of possible applications in quantum information science [1–7], for example, quantum communication and distributed quantum computing. An important class of schemes for quantum communication and computing is based on an elementary process in which single quanta of excitation are transferred back and forth between an atom and a photon [8]. This is achieved within the framework of cavity electrodynamics, which is also the most promising candidate for deterministically producing streams of single photons [9–14] of narrow band and indistinguishable radiation modes [15].

The dissipative dynamics of cavity-atom systems have been well investigated and deeply understood under the Markovian approximation [16]. This approximation is valid when the coupling between the system and the bath is weak such that the perturbation theory can be applied; meanwhile the validity of the Markovian approximation requires that the characteristic time of the bath is sufficiently shorter than that of the system. However, in practice, the coupling of the system to the bath is not weak and the memory effect of the bath cannot be neglected. Typical examples include optical fields propagating in cavity arrays or in an optical fiber [17–19], trapped ions subjected to artificial colored noise [20–22], and microcavities interacting with a coupled resonator optical waveguide or photonic crystals [23–27], to mention a few.

Previous studies of state transfer (or mapping) between atoms and photons in cavity QED are based on the Markovian approximation [28–32]. However, recent studies have shown that Markovian and non-Markovian quantum processes [33–36] play an important role in many fields of physics, e.g., quantum optics [37–39] and quantum information science [40,41]. This motivates us to explore the storing of single photons of arbitrary temporal shape (or a packet) in coupled atom-cavity systems under the non-Markovian approximation.

For this purpose, we first extend the input-output relation in Ref. [31] from a Markovian system to a non-Markovian system [42]. Then we show the difference between Markovian and non-Markovian approximations in the single-photon storing. Next we study state transfer from an input photon state to a

single-photon cavity dark state by adiabatically evolving the system in the non-Markovian regime. The result is compared with that given by the earlier scheme, and we find that these methods are in good agreement with each other.

The remainder of the paper is organized as follows: In Sec. II, we introduce a model to describe the atom-cavity system coupled to input photons and derive the non-Markovian input-output relations; the dynamical equations for the atom-cavity system are also given in this section. In Sec. III, we derive an exact expression for the complex driving pulse with nonzero detunings and nonzero populations of the excited state. In Sec. IV, we study the storing of single photons, taking the non-Markovian processes into account. In Sec. V, we study the adiabatic transfer via dark states between the input photon and the cavity-atom system. Discussion and conclusions are given in Sec. VI.

II. EQUATIONS OF MOTION AND NON-MARKOVIAN INPUT-OUTPUT RELATIONS

We now discuss how to transfer a single-photon state of input field into a single excitation of atom-cavity systems. We consider an effective one-dimensional model, which describes a Fabry-Perot cavity coupled to a three-level atom, as shown in Fig. 1. The input and output fields are parallel to the z axis (perpendicular to the cavity mirrors). The input field partially transmits into the cavity through the mirror at $z = 0$ (the mirror at the right-hand side of the setup), and the other mirror of the cavity is assumed to be 100% reflecting.

The input-output field is introduced as a continuum field modeled by a set of oscillators, denoted by annihilation operator $\hat{b}(\omega)$, which are coupled to the cavity mode with coupling constants $\kappa(\omega)$. The interaction between the cavity field \hat{a} and the continuum $\hat{b}(\omega)$ is described by the following Hamiltonian [30,39,43]:

$$H_{\text{int}} = i \int_{-\infty}^{\infty} d\omega [\kappa(\omega) \hat{a} \hat{b}^{\dagger}(\omega) - \text{H.c.}], \quad (1)$$

where $[b(\omega), b^{\dagger}(\omega')] = \delta(\omega - \omega')$ and $[a, a^{\dagger}] = 1$. We consider an input field in a general single-photon state $|\psi_{\text{in}}(t)\rangle = \int d\omega C_{\omega}^{\text{in}}(t) \hat{b}^{\dagger}(\omega) |0\rangle$ with $C_{\omega}^{\text{in}}(t) = C_{\omega}^{\text{in}}(t_0) e^{-i\omega(t-t_0)}$. Here, $|0\rangle$ denotes the vacuum state of the continuum $b(\omega)$. In what

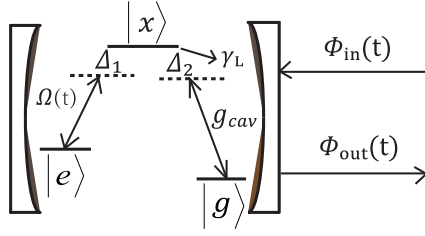


FIG. 1. (Color online) Schematic illustration of our system. It consists of a cavity, a three-level atom, and input-output fields. The atom is driven by both the cavity field with coupling constant g_{cav} and a classical field characterized by the driving pulse $\Omega(t)$. The classical and cavity fields are detuned from the atomic resonance by Δ_1 and Δ_2 , respectively.

follows we characterize these fields by an envelope wave function $\Phi_{in}(z,t)$ defined by

$$\begin{aligned}\Phi_{in}(z,t) &= \int d\omega \langle 0_\omega | \hat{b}(\omega) e^{ikz} | \psi_{in}(t) \rangle \\ &= \int d\omega C_\omega^{in}(t) e^{ikz}.\end{aligned}\quad (2)$$

The normalization condition $\int d\omega |C_\omega^{in}(t)|^2 = 1$ of the Fourier coefficients implies the normalization of the input wave function according to Parseval's theorem:

$$\int dt |\Phi_{in}(z,t)|^2 = 1. \quad (3)$$

Clearly, $\Phi_{in}(z,t)$ describes a single photon propagating along the z axis.

To derive an input-output relation for a general non-Markovian quantum system, we write the total Hamiltonian in a rotation frame with respect to the center frequency ω_c of the cavity field,

$$H = H_S + H_B + H_{int} \quad (4)$$

with

$$H_S = (\Omega(t)e^{i\Delta_1 t} \sigma_{xe} + g_{cav} \sigma_{xg} \hat{a} e^{i\Delta_2 t} + \text{H.c.}) - i\gamma_L \sigma_{xx}, \quad (5)$$

$$H_B = \int_{-\infty}^{\infty} d\omega \Omega_\omega \hat{b}^\dagger(\omega) \hat{b}(\omega),$$

where $\sigma_{\mu\nu} = |\mu\rangle\langle\nu|$ ($\mu, \nu = x, e, g$) are the atomic transition operators, and H.c. stands for the Hermitian conjugate. $|g\rangle$ denotes the ground state with energy $\omega_g = 0$ ($\hbar = 1$, hereafter), and $|e\rangle$ denotes the excited state with energy ω_e . \hat{a} is the annihilation operator of the cavity mode with center frequency ω_c . The $|e\rangle$ to $|x\rangle$ (with energy ω_x) transition is driven by the classical field $\Omega(t)$ with frequency ν_Ω , and the transition from $|g\rangle$ to $|x\rangle$ is driven by the cavity mode with coupling constant g_{cav} . Detuning Δ_1 is defined as $\Delta_1 = \omega_x - \omega_e - \nu_\Omega \equiv \omega_{xe} - \nu_\Omega$, and $\Delta_2 = \omega_x - \omega_g - \omega_c \equiv \omega_{xg} - \omega_c$. γ_L denotes the atomic spontaneous emission rate and $\Omega_\omega = \omega - \omega_c$ the detuning of the ω mode from the center frequency of the cavity.

Assuming there is only one photon initially in the input field and the cavity-atom system is not excited, we can restrict the solution and discussion of the total system (4) to the subspace containing zero and a single excitation. This allows us to expand the state vector of the total system at a later

time t as

$$\begin{aligned}|\psi(t)\rangle &= G(t)|g,1,0\rangle + E(t)|e,0,0\rangle + X(t)|x,0,0\rangle \\ &\quad + \int_{-\infty}^{\infty} d\omega C_\omega(t) \hat{b}^\dagger(\omega) |g,0,0\rangle,\end{aligned}\quad (6)$$

where $|g,1,0\rangle$ denotes a state with the atom in the ground state $|g\rangle$, the cavity having a single photon and no photons in the input. $G(t)$ denotes the probability amplitude of the total system being in $|g,1,0\rangle$. The other states have similar notations. To calculate the probability amplitudes $G(t)$, $E(t)$, $X(t)$, and $C_\omega(t)$, we substitute $|\psi(t)\rangle$ into the Schrödinger equation $i\partial_t |\psi(t)\rangle = H |\psi(t)\rangle$. Simple calculation yields

$$\begin{aligned}\dot{G} &= -ig_{cav} X e^{-i\Delta_2 t} - \int_{-\infty}^{\infty} d\omega \kappa^*(\omega) C_\omega, \\ \dot{E} &= -i\Omega^*(t) e^{-i\Delta_1 t} X, \\ \dot{X} &= -i\Omega(t) e^{i\Delta_1 t} E - ig_{cav} G e^{i\Delta_2 t} - \gamma_L X, \\ \dot{C}_\omega &= -i\Omega_\omega C_\omega + \kappa(\omega) G.\end{aligned}\quad (7)$$

By formally integrating the fourth equation of Eq. (7), we obtain

$$C_\omega(t) = e^{-i\Omega_\omega(t-t_0)} C_\omega(t_0) + \kappa(\omega) \int_{t_0}^t d\tau G(\tau) e^{-i\Omega_\omega(t-\tau)}, \quad (8)$$

where $C_\omega(t_0)$ is the initial condition of $C_\omega(t)$. Similarly,

$$C_\omega(t) = e^{-i\Omega_\omega(t-t_1)} C_\omega(t_1) - \kappa(\omega) \int_t^{t_1} d\tau G(\tau) e^{-i\Omega_\omega(t-\tau)}, \quad (9)$$

where $t_1 \geq t$. The single-photon input and output fields $\Phi_{in}(0,t)$ and $\Phi_{out}(0,t)$ [for simplicity, hereafter we write $\Phi_{out}(0,t)$ as $\Phi_{out}(t)$, the same notation for $\Phi_{in}(t)$] are defined as the Fourier transformation of $C_\omega(t_0)$ and $C_\omega(t_1)$ at $z = 0$, respectively:

$$\begin{aligned}\Phi_{in}(t) &= \frac{-1}{\sqrt{2\pi}} \int_{-\infty}^{\infty} d\omega C_\omega(t_0) e^{-i\Omega_\omega(t-t_0)}, \\ \Phi_{out}(t) &= \frac{1}{\sqrt{2\pi}} \int_{-\infty}^{\infty} d\omega C_\omega(t_1) e^{-i\Omega_\omega(t-t_1)}.\end{aligned}\quad (10)$$

Integrating Eq. (8) and Eq. (9) and using Eq. (10), we obtain a non-Markovian input-output relation (change $t_1 \rightarrow t$)

$$\Phi_{in}(t) + \Phi_{out}(t) = \int_{t_0}^t d\tau h(t-\tau) G(\tau), \quad (11)$$

where

$$h(t) = \frac{1}{\sqrt{2\pi}} \int_{-\infty}^{\infty} d\omega e^{-i\Omega_\omega t} \kappa(\omega) \quad (12)$$

defines the impulse response function that equals the Fourier transform of the coupling strength $\kappa(\omega)$. Substituting Eq. (8) into the first equation of Eq. (7), we obtain finally the general equations of motion for the total system,

$$\begin{aligned}\dot{G} &= -ig_{cav} X e^{-i\Delta_2 t} + N(t) - \int_0^t d\tau f(t-\tau) G(\tau), \\ \dot{E} &= -i\Omega^*(t) e^{-i\Delta_1 t} X, \\ \dot{X} &= -i\Omega(t) e^{i\Delta_1 t} E - ig_{cav} G e^{i\Delta_2 t} - \gamma_L X, \\ \Phi_{in}(t) + \Phi_{out}(t) &= \int_{t_0}^t d\tau h(t-\tau) G(\tau),\end{aligned}\quad (13)$$

where

$$N(t) = \int_{-\infty}^{\infty} d\tau h^*(\tau - t) \Phi_{\text{in}}(\tau) \quad (14)$$

is the driving field,

$$\begin{aligned} f(t - \tau) &= \int_{-\infty}^{\infty} d\zeta h^*(\tau - \zeta) h(t - \zeta) \\ &= \int_{-\infty}^{\infty} d\omega |\kappa(\omega)|^2 e^{-i\Omega_\omega(t-\tau)} \\ &\equiv \int_{-\infty}^{\infty} d\omega J(\omega) e^{-i\Omega_\omega(t-\tau)} \end{aligned} \quad (15)$$

is the memory function of the system, and $J(\omega) = |\kappa(\omega)|^2$. From the derivation, we find that $h(t)$ and $f(t)$ plays essential roles in the photon storing. Different $h(t)$ and $f(t)$ leads to different non-Markovianity of the dynamics; hence they affect the design of the driving pulse to store a photon in the atom-cavity system.

III. DRIVING PULSE AND EXCITED-STATE POPULATION

In this section we present an analytical expression for the driving pulse to completely store an arbitrary photon wave packet $\Phi_{\text{in}}(t)$ in the atom-cavity system. Obviously, complete impedance matching is a necessary condition for this purpose, i.e.,

$$\Phi_{\text{out}}(t) = 0 \quad (16)$$

must be satisfied at any time.

The spectral response function $\kappa(\omega)$ for the Fabry-Perot (FP) cavity can be defined by

$$\kappa(\omega) = \sqrt{\frac{\Gamma}{2\pi}} \frac{W}{W - i(\omega - \omega_c)}, \quad (17)$$

where Γ is the cavity-input coupling strength and W is the spectrum bandwidth of the input field. The effective spectral density is then [45–47]

$$J(\omega) = \frac{\Gamma}{2\pi} \frac{W^2}{W^2 + (\omega - \omega_c)^2}. \quad (18)$$

In the wide-band limit (i.e., $W \rightarrow \infty$), the spectral density approximately takes $J(\omega) \rightarrow \frac{\Gamma}{2\pi}$, equivalently, $\kappa(\omega) \rightarrow \sqrt{\frac{\Gamma}{2\pi}}$. This describes the case in the Markovian limit. Then according to Eqs. (12) and (15) we have

$$h(t) = \sqrt{\Gamma} \delta(t), \quad f(t) = \Gamma \delta(t). \quad (19)$$

Substituting Eq. (19) into Eq. (13), we obtain the Markovian dynamics of the total system [28,31]:

$$\begin{aligned} \dot{G} &= -i g_{\text{cav}} X e^{-i\Delta_2 t} + \sqrt{\Gamma} \Phi_{\text{in}}(t) - \frac{1}{2} \Gamma G(t), \\ \dot{E} &= -i \Omega^*(t) e^{-i\Delta_1 t} X, \\ \dot{X} &= -i \Omega(t) e^{i\Delta_1 t} E - i g_{\text{cav}} G e^{i\Delta_2 t} - \gamma_L X, \end{aligned} \quad (20)$$

$$\Phi_{\text{in}}(t) + \Phi_{\text{out}}(t) = \sqrt{\Gamma} G(t).$$

In order to take the non-Markovian effect into account, we calculate the system-field memory function $f(t)$ and

the spectral-response function $h(t)$ [46,48,49] by the use of Eqs. (17) and (18). They read

$$h(t) = W \sqrt{\Gamma} \Theta(t) e^{-Wt} \quad (21)$$

and

$$f(t) = \frac{1}{2} W \Gamma e^{-W|t|}, \quad (22)$$

where $\Theta(t)$ is the unit step function

$$\Theta(t) = \begin{cases} 1, & t \geq 0, \\ 0, & t \leq 0. \end{cases}$$

To store an input photon into the atom-cavity system, it is reasonable to assume that the total system is initially prepared in state $\hat{b}^\dagger(\omega)|g, 0, 0\rangle$, i.e., the initial condition for the equations of motion is

$$\int dt |\Phi_{\text{in}}(t)|^2 = 1, \quad (23)$$

$$G(0) = 0, \quad (24)$$

$$X(0) = 0, \quad (25)$$

$$E(0) = 0. \quad (26)$$

Now we calculate the population of the atom in the excited state $|e, 0, 0\rangle$,

$$\begin{aligned} \rho_{ee}(t) &= \rho_{\text{offset}} - \tilde{X}^2(t) \\ &+ \int_0^t dt' [2g_{\text{cav}} \tilde{X}(t') G(t') - 2\gamma_L \tilde{X}^2(t')]. \end{aligned} \quad (27)$$

Equation (27) shows that the population of excited state $\rho_{ee}(t)$ does not depend on the detunings Δ_1 and Δ_2 . From the derivation below for the complex driving pulse $\Omega(t)$, we see that we should introduce an offset term ρ_{offset} phenomenologically to account for the imperfect state preparation—a small initial population in the excited state $|e, 0, 0\rangle$. The derivations of Eq. (27) are given in Appendix; for details, see Appendix.

We now proceed to derive the complex driving pulse $\Omega(t)$ for completely storing a photon in arbitrary temporal shape with nonzero detunings Δ_1 and Δ_2 ,

$$\Omega(t) = \alpha(t) + i\beta(t), \quad (28)$$

where

$$\begin{aligned} \alpha(t) &= [\partial_t \tilde{X}(t) \cos A(t) - g_{\text{cav}} G(t) \cos A(t) \\ &+ \gamma_L \tilde{X}(t) \cos A(t) + \Delta_2 \tilde{X}(t) \sin A(t)] / \sqrt{\rho_{ee}(t)}, \\ \beta(t) &= [\Delta_2 \tilde{X}(t) \cos A(t) - \partial_t \tilde{X}(t) \sin A(t) + g_{\text{cav}} G(t) \sin A(t) \\ &- \gamma_L \tilde{X}(t) \sin A(t)] / \sqrt{\rho_{ee}(t)}, \end{aligned} \quad (29)$$

with

$$A(t) = -\Delta \cdot t + \Delta_2 \int_0^t dt' \frac{\tilde{X}^2(t')}{\rho_{ee}(t')}. \quad (30)$$

The details of the derivation of Eq. (28) can be found in Appendix.

The modulus and argument of the complex driving pulse $\Omega(t) = |\Omega(t)| e^{i\theta(t)}$ are

$$|\Omega(t)| = \sqrt{\alpha^2(t) + \beta^2(t)} \quad (31)$$

$$= \sqrt{\frac{[\partial_t \tilde{X}(t) - g_{\text{cav}} G(t) + \gamma_L \tilde{X}(t)]^2 + \Delta_2^2 \tilde{X}(t)^2}{\rho_{ee}(t)}}, \quad (32)$$

$$\theta(t) = \arctan \left[\frac{\beta(t)}{\alpha(t)} \right], \quad (33)$$

which is an analytical expression that defines the complex driving pulse necessary to completely store the desired photon packet. This equation tells us that the modulus of the driving pulse $\Omega(t)$ depends only on the detuning Δ_2 , not on the detuning Δ_1 .

Under the Markovian approximation (we denote the quantities in the Markovian case by introducing a subscript f to them) and defining $X_f(t) = -ie^{i\Delta_2 t} \tilde{X}_f(t)$ and $E_f(t) = e^{-i\Delta_1 t + i\Delta_2 t} \tilde{E}_f(t)$, we obtain from Eq. (20) the following results with nonzero Δ_1 and Δ_2 :

$$\begin{aligned} G_f(t) &= \Phi_{\text{in}}(t)/\sqrt{\Gamma}, \\ \tilde{X}_f(t) &= \left[-\dot{G}_f(t) + \frac{1}{2}\Gamma G_f(t) \right] / g_{\text{cav}}, \\ \rho_{\text{fee}} &= \rho_{\text{offset}} - \tilde{X}_f^2 \\ &\quad + \int_0^t dt' [2g_{\text{cav}} \tilde{X}_f(t') G_f(t') - 2\gamma_L \tilde{X}_f^2(t')], \\ \Omega_f(t) &= \alpha_f(t) + i\beta_f(t), \end{aligned} \quad (34)$$

where

$$\begin{aligned} \alpha_f(t) &= [\cos(A_f) \partial_t \tilde{X}_f - g_{\text{cav}} \cos(A_f) G_f \\ &\quad + \gamma_L \cos(A_f) \tilde{X}_f + \Delta_2 \sin(A_f) \tilde{X}_f] / \sqrt{\rho_{\text{fee}}}, \\ \beta_f(t) &= [\Delta_2 \cos(A_f) \tilde{X}_f - \sin(A_f) \partial_t \tilde{X}_f \\ &\quad + g_{\text{cav}} \sin(A_f) G_f - \gamma_L \sin(A_f) \tilde{X}_f] / \sqrt{\rho_{\text{fee}}}, \\ A_f(t) &= -\Delta \cdot t + \Delta_2 \int_0^t dt' \frac{\tilde{X}_f^2(t')}{\rho_{\text{fee}}(t')}. \end{aligned} \quad (35)$$

Within the Markovian approximation, the modulus $|\Omega_f(t)|$ and argument $\theta_f(t)$ of the complex driving pulse $\Omega_f(t)$ can be written in the same form as in Eqs. (31) and (33), by replacing $\alpha(t)$ by $\alpha_f(t)$ and $\beta(t)$ by $\beta_f(t)$. This driving pulse representing the coupling constant between the atom and the driving fields is complex when the detunings are not zero, which is not discussed in the earlier studies.

IV. SINGLE-PHOTON STORING AND IMPEDANCE MATCHING

We now consider a realistic input photon packet that starts from time t_0 and ends at time t_e . We assume the packet starts off smoothly, i.e., $\Phi_{\text{in}}(t_0) = \partial_t \Phi_{\text{in}}(t_0) = 0$, as described in [44]. The second time derivative of the input $\Phi_{\text{in}}(t_0)$ might be nonzero at t_0 ; thus $G(0) = 0$ in Eq. (A1), but

$$\dot{G}(t_0) = \frac{\ddot{\Phi}_{\text{in}}(t_0)}{W\sqrt{\Gamma}} \neq 0. \quad (36)$$

Furthermore, from Eq. (A2) together with Eqs. (25) and (24) we find

$$\dot{G}(0) = N(0), \quad (37)$$

the so-called equilibrium condition.

By Eqs. (14) and (21) we can establish a relation between W and Γ for arbitrary input photon wave packets Φ_{in} ,

$$\Gamma = \frac{\ddot{\Phi}_{\text{in}}(0)}{W^2 \int_t^\infty d\tau e^{-W(\tau-t)} \Phi_{\text{in}}(\tau)}. \quad (38)$$

We should notice that the initial conditions from Eq. (28) now become $A(0) = 0$, $\beta(0) = 0$, and $\Omega(0) = \alpha(0) = \frac{\partial_t \tilde{X}(0)}{\sqrt{\rho_{\text{offset}}}} \neq 0$. To satisfy the last initial condition, a small but nonvanishing initial population in the state $|g, 0, 0\rangle$ is required, in other words, perfect impedance matching with $\rho_{\text{offset}} = 0$ would only be possible when the input photon packet lasts for a very long (infinite) time.

To exemplify the scheme and discuss the implications of the constraints to the initial population, we now apply the design to a couple of typical photon shapes (or packets) that are of general interest. First, we consider photon wave packets on a finite support ranging from 0 to T symmetric in time. A particular normalization shape (or packets) that meets the above initial condition is

$$\Phi_{\text{in}}(t) = \frac{8\sin^2(2t\pi/T)\cos^2(t\pi/T)}{\sqrt{7\pi}}. \quad (39)$$

Taking $T = \pi\mu s$, we obtain a constraint on W and Γ in the input packet from Eq. (38):

$$\Gamma = \frac{(W^2 + 4)(W^2 + 16)(W^2 + 36)}{W(W^4 + 28W^2 + 72)(1 - e^{-\pi W})}. \quad (40)$$

Notice the unit step function in $h(t)$; the upper and lower limits of the integral in Eq. (14) are T and t , respectively. For zero detunings, $\Delta_1 = \Delta_2 = 0$, the driving pulse $\Omega(t)$ (28) is real. This together with Eqs. (29) and (30) yields $A(t) = 0$, $\beta(t) = 0$ and a real $\alpha(t)$:

$$\Omega(t) = \alpha(t) = [\partial_t \tilde{X}(t) - g_{\text{cav}} G(t) + \gamma_L \tilde{X}(t)] / \sqrt{\rho_{ee}}. \quad (41)$$

For an input photon packet with a duration of $T = \pi\mu s$, we plot $\Phi_{\text{in}}(t)$, $\Omega(t)$, and the probability amplitude of reflected photon $\Phi_{\text{out}}(t)$ as a function of time in Fig. 2. $\Phi_{\text{out}}(t)$ is obtained from numerical simulations of Eq. (13) for the following two cases: (1) the system is initially prepared in $|g, 0, 0\rangle$, i.e., $\rho_{\text{offset}} = 0$; and (2) the population of the atom in the excited state is initially not zero (in the figure we choose $\rho_{\text{offset}} = 0.002$), while the cavity is empty. We emphasize that in the numerical simulations here and hereafter, the frequency is rescaled in units of megahertz, and accordingly the time t is in units of microseconds. To be specific, we choose $g_{\text{cav}} = 30\pi$ MHz and $\gamma_L = 6\pi$ MHz to plot Fig. 2. This choice of parameters was suggested in [31,44], which is within reach of current technologies. Note that in this plot we use the same driving pulse $\Omega(t)$, which is calculated with $\rho_{\text{offset}} = 0.002$. We should emphasize that the choice of ρ_{offset} is arbitrary and limited only by practical considerations; we will discuss this issue again later.

Figures 2(a) and 2(b) show that in order to store the input photon completely, we have to change the driving pulse according to the cavity-input field couplings. From Fig. 2(c) we can learn that when the initial state of an atom matches the conditions used to calculate $\Omega(t)$, i.e., with $\rho_{\text{offset}} = 0.002$, no photon is reflected out (it is below 10^{-16} , almost zero).

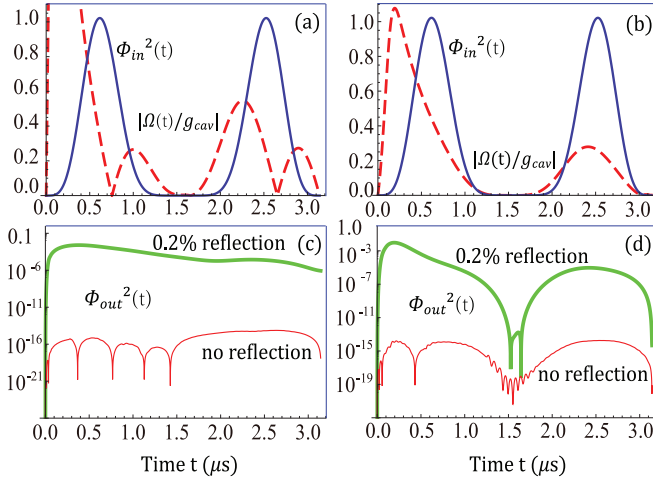


FIG. 2. (Color online) Input single-photon packet (blue line), the driving pulse (red-dashed line), and $|\Phi_{out}|^2$ as a function of time. The parameters chosen are $g_{cav} = 30\pi$ MHz, $\gamma_L = 6\pi$ MHz. In the numerical simulations here and hereafter, the coupling strength Γ is given by Eq. (40). Initially, the system is prepared almost in $|g, 0, 0\rangle$ with a small probability $\rho_{offset} = 0.002$ in $|e, 0, 0\rangle$, which is plotted in (c) and (d) (thin red lines). For comparison, we plot $|\Phi_{out}|^2$ in (c) and (d) (bold green lines) for the case in which the system is prepared with probability 1 in $|g, 0, 0\rangle$. Note that in this case, we still use the driving pulse calculated with $\rho_{offset} = 0.002$, so the reflection is higher. The other parameters chosen are $\Delta_1 = \Delta_2 = 0$, $W = 1.6716$ MHz for (a) and (c), $W = 17.238$ MHz for (b) and (d).

However, if the initial state deviates from the state used to calculate the driving pulse, say the initial state is $|g, 0, 0\rangle$, the photon would be reflected off the cavity with an probability of 0.2%, which is much larger than 10^{-16} and can be explained as a mismatch between the initial state used to calculate the driving pulse and the realistic initial state.

In order to compare the results of the non-Markovian process with that of the Markovian process, we plot the time evolution of the atomic population in the excited state $|e\rangle$ and the real driving pulse (corresponding to zero detunings) $\Omega(t)$ (41) in Fig. 3. We find that when the coupling W is small [see Figs. 3(a) and 3(c)], the so-called backflowing phenomenon occurs for the population ρ_{ee} . As W increases, the results given by the non-Markovian equation (27) are in good agreement with those given in the Markovian limit [see Figs. 3(b) and 3(d)]. Besides, from Figs. 4(a) and 4(b), we can see that the excited-state population $\rho_{ee}(t)$ obtained in the non-Markovian case [Eq. (27)] is different from that $\rho_{fee}(t)$ in the Markovian case [Eq. (34)] when the parameter W runs from 0.5 to 2, but the difference is not clear for $W > 2$ [see Figs. 4(c) and 4(d)].

To shed more light on the photon storing in the non-Markovian limit, we compare the non-Markovian results with those in the Markovian case [see Fig. 5(a)]. By the input signal $|\Phi_{in}|^2$, we divide the dynamics and the time dependence of the driving pulse into four regimes, labeled I–IV. In regimes I and III, the driving pulse $\Omega(t)$ is negative in both non-Markovian and Markovian cases, while the populations of the atom in the excited state $|e\rangle$ increase continuously in these regimes, i.e., no population backflow in the dynamics. In contrary, the driving

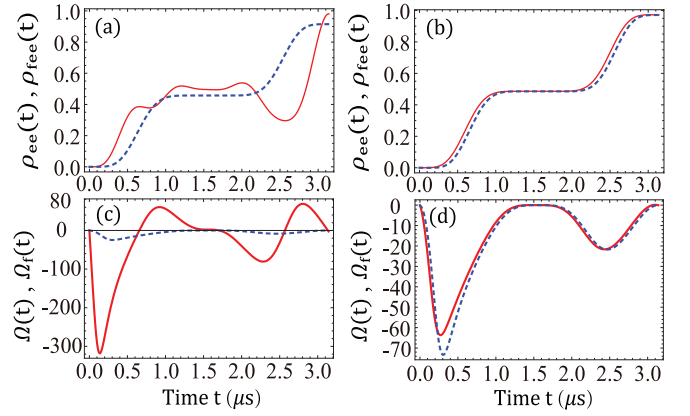


FIG. 3. (Color online) The populations of the atom on the excited state $\rho_{ee}(t)$ (non-Markovian case) and $\rho_{fee}(t)$ (Markovian case), the driving pulse $\Omega(t)$ (non-Markovian case) and $\Omega_f(t)$ (Markovian case) versus time t . The red line denotes the non-Markovian case and the blue-dashed line denotes the Markovian case. Parameters chosen are $\Delta_1 = \Delta_2 = 0$, $\rho_{offset} = 0.0075$, $g_{cav} = 30\pi$ MHz, $\gamma_L = 6\pi$ MHz, $W = 0.5$ MHz, for (a) and (c), $W = 25$ MHz for (b) and (d).

pulse in regimes II and IV are positive, and there is population backflow in these regimes.

Now we study the effect of detunings Δ_1 and Δ_2 on the driving pulse $\Omega(t)$. Examining Eq. (29), we find that $A(t) = \Delta_1 t$ and $\Omega(t) = e^{-i\Delta_1 t} [\partial_t \tilde{X}(t) - g_{cav} G(t) + \gamma_L \tilde{X}(t)]$ when the detuning $\Delta_2 = 0$. When $\Delta_2 \neq 0$, the modulus $|\Omega(t)|$ of the driving pulse $\Omega(t)$ does not depend on the detuning Δ_1 , while it depends on the absolute value of Δ_2 only (see Fig. 6). Meanwhile, the argument $\theta(t)$ of the $\Omega(t)$ depends on both detunings Δ_1 and Δ_2 . The argument $\theta(t)$ of the driving pulse $\Omega(t)$ is an odd function of Δ_2 [see Figs. 7(a) and 7(b)] when $\Delta_1 = 0$ or $\Delta_1 = \Delta_2$.

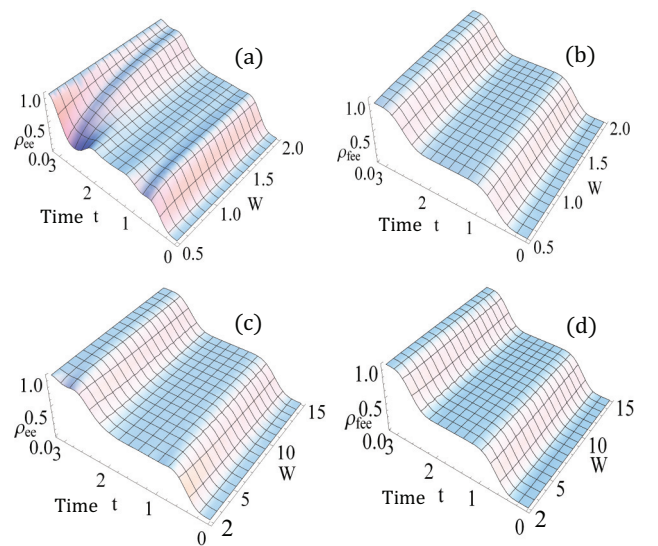


FIG. 4. (Color online) The time evolution of the excited-state population in non-Markovian limit $\rho_{ee}(t)$ and in the Markovian limit $\rho_{fee}(t)$ as a function of time t and the coupling strength W . Parameters chosen are $g_{cav} = 30\pi$ MHz, $\gamma_L = 6\pi$ MHz.

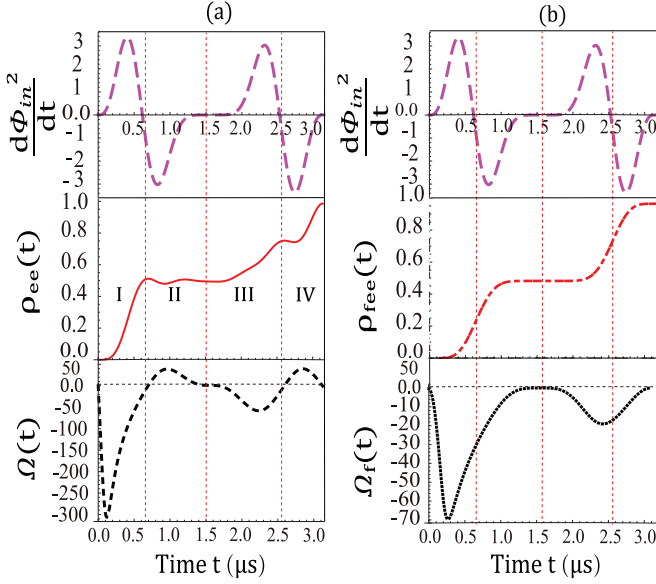


FIG. 5. (Color online) Comparison of non-Markovian case to a Markovian case in terms of $\rho(t)$ and $\Omega(t)$. Parameters chosen are $\Delta_1 = \Delta_2 = 0$, $g_{\text{cav}} = 30\pi$ MHz, $\gamma_L = 6\pi$ MHz, $W = 1$ MHz, $\rho_{\text{offset}} = 0.004$.

V. PHOTON STORING IN DARK STATES

We now discuss the problem of transferring a single-photon state of the input field to an atom-cavity dark state, taking the non-Markovian effect into account. We show that these processes can be achieved by adiabatically rotating the cavity dark state in a special way. Before proceeding, we introduce a dark $|D(t)\rangle$ and its orthogonal bright states $|B(t)\rangle$ [30,50]:

$$\begin{aligned} |D(t)\rangle &= -\cos\varphi(t)|g,1,0\rangle + \sin\varphi(t)|e,0,0\rangle, \\ |B(t)\rangle &= \sin\varphi(t)|g,1,0\rangle + \cos\varphi(t)|e,0,0\rangle, \end{aligned} \quad (42)$$

where $\tan\varphi(t) = g_{\text{cav}}/\Omega(t)$.

Taking the dark and bright states instead of $|g,1,0\rangle$ and $|e,0,0\rangle$ as the basis, we re-expand Eq. (43) as

$$\begin{aligned} |\psi(t)\rangle &= D(t)|D(t)\rangle + B(t)|B(t)\rangle + X(t)|x,0,0\rangle \\ &+ \int_{-\infty}^{\infty} d\omega C_{\omega}(t)\hat{b}^{\dagger}(\omega)|g,0,0\rangle. \end{aligned} \quad (43)$$

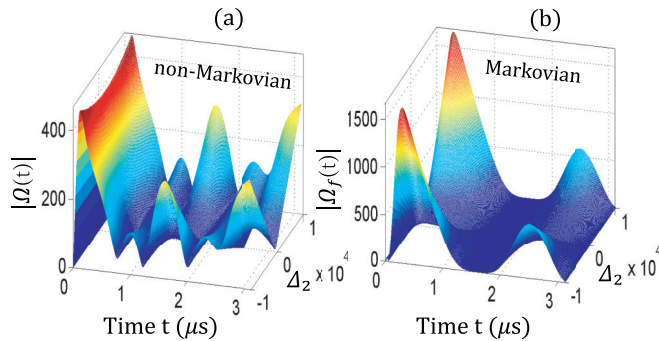


FIG. 6. (Color online) The modulus $|\Omega(t)|$ [non-Markovian case, see Eq. (32)] and $|\Omega_f(t)|$ (Markovian case) of the driving pulse $\Omega(t)$ vary with the detuning Δ_2 and time t . Parameters chosen are $g_{\text{cav}} = 30\pi$ MHz, $\gamma_L = 6\pi$ MHz, $W = 0.5$ MHz, $\rho_{\text{offset}} = 0.003$.

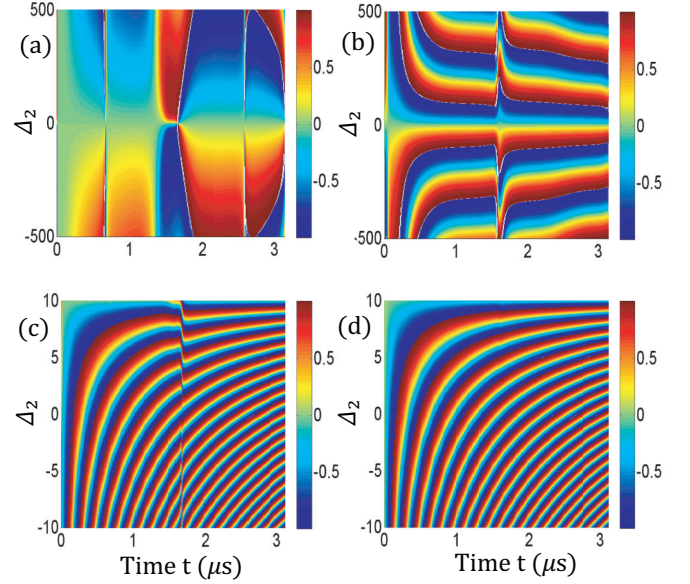


FIG. 7. (Color online) The argument $\sin\theta(t)$ [(a) and (c), see Eq. (33)] in the non-Markovian case and $\sin\theta_f(t)$ [(b) and (d)] in the Markovian case vary with the detuning Δ_2 and time t . Parameters chosen are $\Delta_1 = \Delta_2$, $g_{\text{cav}} = 30\pi$ MHz, $\gamma_L = 6\pi$ MHz, $W = 0.5$ MHz, $\rho_{\text{offset}} = 0.003$ for (a) and (b), and $\Delta_1 = 20$ for (c) and (d).

The relations between the amplitudes $D(t)$, $B(t)$, $G(t)$, and $E(t)$ can be written as

$$\begin{aligned} D(t) &= -\cos\varphi(t)G(t) + \sin\varphi(t)E(t), \\ B(t) &= \sin\varphi(t)G(t) + \cos\varphi(t)E(t). \end{aligned} \quad (44)$$

The evolution equations (7) in terms of Eq. (44) then take (we here consider only $\Delta_1 = \Delta_2 = 0$)

$$\begin{aligned} \dot{X} &= -i\Omega_1(t)B(t) - \gamma_L X, \\ \dot{D} &= \dot{\varphi}B(t) + \cos\varphi \int d\omega \kappa^*(\omega)C_{\omega}, \\ \dot{B} &= -\dot{\varphi}D(t) - i\Omega_1(t)X - \sin\varphi \int d\omega \kappa^*(\omega)C_{\omega}, \\ \dot{C}_{\omega} &= -i\Omega_{\omega}C_{\omega} + \kappa(\omega)\sin\varphi B(t) - \cos\varphi\kappa(\omega)D(t), \end{aligned} \quad (45)$$

where $\Omega_1(t) = \sqrt{g_{\text{cav}}^2 + \Omega^2(t)}$, and the terms proportional to $\dot{\varphi}$ describe the coupling between the bright and dark state induced by nonadiabatic evolutions. We now adiabatically eliminate the excited state, which is possible if the characteristic time t_1 of the system is sufficiently longer than the decay time of the excited state ($\gamma_L t_1 \gg 1$). After elimination of the excited state, we adiabatically eliminate the bright state and neglect terms with $\dot{\varphi}$. The conditions which validate such an elimination will be given later. Defining $D(t) = -d_1$, we finally arrive at [29,30]

$$\begin{aligned} \dot{d}_1 &= -\cos\varphi(t) \int d\omega \kappa^*(\omega)C_{\omega}(t), \\ \dot{C}_{\omega} &= -i\Omega_{\omega}C_{\omega}(t) + \cos\varphi(t)\kappa(\omega)d_1(t). \end{aligned} \quad (46)$$

One immediately recognizes from these equations that the total probability of finding the system in single-photon states of the

input field and in the cavity-dark state is conserved:

$$\frac{d}{dt} \left[|d_1(t)|^2 + \int d\omega |C_\omega(t)|^2 \right] = 0. \quad (47)$$

Thus with adiabatic evolution, the system can occupy only two states, namely, the input field state and the cavity dark state.

By formally integrating the second equation of Eq. (46) and substituting it into the first [these steps are similar to Eqs. (7)–(13)], we get

$$\begin{aligned} \dot{d}_1(t) &= \cos \varphi(t) N(t) - \cos \varphi(t) \\ &\quad \times \int_0^t d\tau \cos \varphi(\tau) d_1(\tau) f(t - \tau), \\ \Phi_{\text{in}}(t) + \Phi_{\text{out}}(t) &= \int_0^t d\tau h(t - \tau) \cos \varphi(\tau) d_1(\tau). \end{aligned} \quad (48)$$

We note the adiabatic evolution happens when [6,29,30]

$$g_{\text{cav}}^2 \gg \gamma_L \Gamma. \quad (49)$$

This condition is the same as that for adiabatic storing in the Markovian limit, in other words, the non-Markovian and Markovian systems share the same condition to store a photon adiabatically. Making use of the completely impedance matching condition Eq. (16), we obtain

$$\cos \varphi(t) d_1(t) = G(t). \quad (50)$$

By substituting Eq. (50) into the first equation of Eq. (48), we get

$$d_1(t) = \sqrt{2 \int_0^t M(\tau) d\tau}, \quad \Omega(t) = \frac{g_{\text{cav}}}{\tan \varphi(t)}, \quad (51)$$

where $M(t) = G(t)N(t) - G(t) \int_0^t G(\tau) f(t - \tau) d\tau$, $\cos \varphi(t) = \frac{G(t)}{d_1(t)}$. In order to compare the analytical results under the adiabatic evolution Eq. (51) with the exact analytical results in Eq. (41) given by

$$D_{\text{dark}}(t) = G(t) \cos \varphi_1(t) - E(t) \sin \varphi_1(t), \quad (52)$$

we plot the time evolution of the population of the dark state and the driving pulse in Fig. 8. Here $G(t)$ and $E(t) = \sqrt{\rho_{ee}(t)}$ are the exact analytical expressions in Eq. (A1) and Eq. (27), respectively, and $\varphi_1 = \arctan[g_{\text{cav}}/\Omega(t)]$ is determined by Eq. (41).

We find from the figure that the results given by the adiabatic elimination Eq. (51) are in good agreement with those obtained by the exact analytical expression Eq. (41) and Eq. (52) when the strong coupling conditions (49) are satisfied [see Figs. 8(a), 8(c), and 8(b), 8(d)]. When the coupling is weak (49) [see Figs. 8(e) and 8(f)], the curve obtained by the adiabatic elimination approximation Eq. (51) has serious deviations from those obtained by the exact analytical expression Eqs. (41) and (52). In addition, from Figs. 8(b), 8(d), and 8(f), we can see that the driving pulse $\Omega(t)$ obtained by the adiabatic elimination Eq. (51) shows serious deviations from those obtained by the exact analytical expression Eq. (41) when the time is short (approximately $t = 0.2 \mu\text{s}$). This can be explained as an effect of the imperfect impedance matching, in other words, with $\rho_{\text{offset}} = 0$ the perfect impedance matching can take place only with $\Omega(t) \rightarrow \infty$.

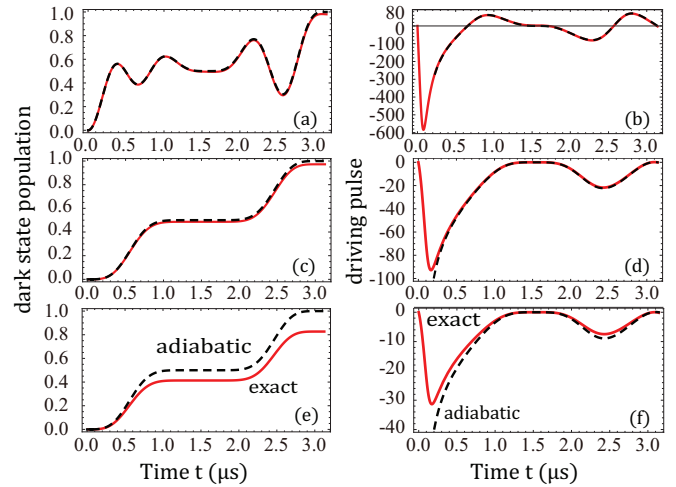


FIG. 8. (Color online) This plot shows the comparison of the adiabatic elimination approximation and the exact expression. The red line and black-dashed line denote the exact solution [see Eqs. (52) and (41)] and the solution of the adiabatic elimination approximation [see Eq. (51)]. Parameters chosen are $\Delta_1 = \Delta_2 = 0$, $\rho_{\text{offset}} = 0.00075$, $g_{\text{cav}} = 30\pi$ MHz, $\gamma_L = 6\pi$ MHz, $W = 0.5$ MHz for (a) and (b); $g_{\text{cav}} = 30\pi$ MHz, $\gamma_L = 6\pi$ MHz, $W = 25$ MHz for (c) and (d); and $g_{\text{cav}} = 14\pi$ MHz, $\gamma_L = 6\pi$ MHz, $W = 25$ MHz for (e) and (f).

From Figs. 8(a) and 8(b), we can learn that the non-Markovianity-caused backflow to the dark state occurs when the parameter W is small. The non-Markovian regime transits to the Markovian regime when the parameter W is large. Therefore by manipulating W we can control the crossover from a non-Markovian process to a Markovian process and vice versa, which provides us with photon storage in the atom-cavity system in both non-Markovian and Markovian limits.

VI. CONCLUSION

The storing of a single photon of arbitrary temporal shape in a single three-level atom coupled to an optical cavity in non-Markovian dynamics has been explored. To calculate the driving pulse, we first extend the input-output relation from a Markovian to non-Markovian process, taking the off-resonant couplings between the atom and fields into account. With the extended input-output relation, we have presented a very simple recipe for calculating the driving pulse with nonzero detunings Δ_1 and Δ_2 , and discuss the features caused by the non-Markovian effect. The results show that the driving field might take different sign at different times for the non-Markovian case, while it is always negative in the Markovian case. From the respect of atoms, there is a backflow in the population on the excited state in the non-Markovian case, whereas there is no backflow in the Markovian case. The fidelity to store a photon in the cavity can reach 1 for both cases, regardless of whether the process is Markovian or non-Markovian. We also present a proposal to store the single photon in a dark state of the cavity-atom system by adiabatically steering the dark state.

ACKNOWLEDGMENT

This work is supported by the NSF of China under Grants No. 61078011, No. 10935010, and No. 11175032.

APPENDIX: DERIVATION OF THE POPULATION OF THE ATOM IN THE EXCITED STATE AND THE COMPLEX DRIVING PULSE WITH DETUNINGS

1. The population of the atom in the excited state

By substituting Eqs. (21) and (16) into the first and fourth equation of Eq. (13), we obtain

$$G(t) = \frac{\dot{\Phi}_{\text{in}}(t) + W\Phi_{\text{in}}(t)}{W\sqrt{\Gamma}} \quad (\text{A1})$$

and

$$\tilde{X}(t) = \left[-\dot{G}(t) + N(t) - \int_0^t d\tau f(t-\tau)G(\tau) \right] / g_{\text{cav}}, \quad (\text{A2})$$

where $\tilde{X}(t) = ie^{-i\Delta_2 t} X(t)$. We note that the envelope $\Phi_{\text{in}}(t)$ of the input is a real function of time, so both $G(t)$ and \tilde{X} are real. Defining $E(t) = e^{-i\Delta_1 t + i\Delta_2 t} \tilde{E}(t)$, we have from Eq. (7)

$$\Omega(t)\tilde{E}(t) = \partial_t \tilde{X}(t) + i\Delta_2 \tilde{X}(t) - g_{\text{cav}}G(t) + \gamma_L \tilde{X}(t) \quad (\text{A3})$$

and

$$\Omega^*(t)\tilde{X}(t) = -i\Delta \tilde{E}(t) - \partial_t \tilde{E}(t), \quad (\text{A4})$$

where $\Delta = \Delta_2 - \Delta_1$. It is easy to see that $\tilde{E}(t)$ and $\Omega(t)$ are complex due to nonzero detunings Δ_1 and Δ_2 ; this is one of the differences between our work and the earlier work [31]. Taking a complex conjugation of both sides of Eq. (A3) yields

$$\Omega(t)^* \tilde{E}^*(t) = \partial_t \tilde{X}(t) - i\Delta_2 \tilde{X}(t) - g_{\text{cav}}G(t) + \gamma_L \tilde{X}(t). \quad (\text{A5})$$

Dividing Eq. (A4) by Eq. (A5), we have

$$\begin{aligned} & -i\Delta |E(t)|^2 - \tilde{E}^*(t)\partial_t \tilde{E}(t) \\ & = \tilde{X}(t)\partial_t \tilde{X}(t) - i\Delta_2 \tilde{X}^2(t) - g_{\text{cav}}\tilde{X}(t)G(t) + \gamma_L \tilde{X}^2(t). \end{aligned} \quad (\text{A6})$$

Taking the complex conjugation of both sides of Eq. (A4), we have

$$\Omega(t)\tilde{X}(t) = i\Delta \tilde{E}^*(t) - \partial_t \tilde{E}^*(t). \quad (\text{A7})$$

Dividing Eq. (A3) by Eq. (A7), we have

$$\begin{aligned} & -i\Delta |E(t)|^2 + \tilde{E}(t)\partial_t \tilde{E}^*(t) \\ & = -\tilde{X}(t)\partial_t \tilde{X}(t) - i\Delta_2 \tilde{X}^2(t) + g_{\text{cav}}\tilde{X}(t)G(t) - \gamma_L \tilde{X}^2(t). \end{aligned} \quad (\text{A8})$$

Using Eq. (A8), Eq. (A6), and $\partial_t \rho_{ee}(t) = \tilde{E}(t)\partial_t \tilde{E}^*(t) + \tilde{E}^*(t)\partial_t \tilde{E}(t)$, we get a differential equation of $\rho_{ee}(t)$

$$\dot{\rho}_{ee}(t) = -2\tilde{X}(t)\partial_t \tilde{X}(t) + 2g_{\text{cav}}\tilde{X}(t)G(t) - 2\gamma_L \tilde{X}^2(t). \quad (\text{A9})$$

Therefore, Eq. (27) can be obtained by formally integrating Eq. (A9).

2. The complex driving pulse with detunings

Multiplying both sides of Eq. (A8) by $-i$ and taking the complex conjugation of the result, we obtain

$$\begin{aligned} & -\Delta |\tilde{E}(t)|^2 + i\tilde{E}^*(t)\partial_t \tilde{E}(t) \\ & = -i\tilde{X}(t)\partial_t \tilde{X}(t) - \Delta_2 \tilde{X}^2(t) + ig_{\text{cav}}\tilde{X}(t)G(t) - i\gamma_L \tilde{X}^2(t). \end{aligned} \quad (\text{A10})$$

Considering

$$\tilde{E}^*(t) = \frac{\rho_{ee}(t)}{\tilde{E}(t)}, \quad \rho_{ee}(t) = |\tilde{E}(t)|^2, \quad (\text{A11})$$

substituting Eq. (A11) into Eq. (A10), and formally integrating the obtained result from 0 to t , we arrive at

$$\begin{aligned} \tilde{E}(t) = \tilde{E}(0) \exp \int_0^t dt' \{ & [\Delta \rho_{ee}(t') - i\tilde{X}(t')\partial_{t'} \tilde{X}(t') - \Delta_2 \tilde{X}^2(t') \\ & + ig_{\text{cav}}\tilde{X}(t')G(t') - i\gamma_L \tilde{X}^2(t')]/i\rho_{ee}(t') \}, \end{aligned} \quad (\text{A12})$$

where $\tilde{E}(0) = \sqrt{\rho_{\text{offset}}}$ represents the initial offset, i.e., the probability amplitude of finding the system in the excited state. Finally, we can obtain Eq. (28) by substituting Eq. (A12) into Eq. (A3) and separating the real and imaginary part of the complex driving pulse $\Omega(t)$.

-
- [1] D. P. DiVincenzo, *Nature (London)* **393**, 113 (1998).
 [2] E. Knill, R. Laflamme, and G. J. Milburn, *Nature (London)* **409**, 46 (2001).
 [3] J. I. Cirac, A. K. Ekert, S. F. Huelga, and C. Macchiavello, *Phys. Rev. A* **59**, 4249 (1999).
 [4] D. P. DiVincenzo, *Fortschr. Phys.* **48**, 771 (2000).
 [5] J. I. Cirac, P. Zoller, H. J. Kimble, and H. Mabuchi, *Phys. Rev. Lett.* **78**, 3221 (1997).
 [6] L.-M. Duan, A. Kuzmich, and H. J. Kimble, *Phys. Rev. A* **67**, 032305 (2003).
 [7] R.-B. Liu, W. Yao, and L. J. Sham, *Adv. Phys.* **59**, 703 (2010).
 [8] M. Oxborrow and A. G. Sinclair, *Contemp. Phys.* **46**, 173 (2005).
 [9] C. K. Law and H. J. Kimble, *J. Mod. Opt.* **44**, 2067 (1997).
 [10] A. Kuhn, M. Hennrich, T. Bundo, and G. Rempe, *Appl. Phys. B* **69**, 373 (1999).
 [11] A. Kuhn, M. Hennrich, and G. Rempe, *Phys. Rev. Lett.* **89**, 067901 (2002).
 [12] B. Sun, M. S. Chapman, and L. You, *Phys. Rev. A* **69**, 042316 (2004).
 [13] J. McKeever, A. Boca, A. D. Boozer, R. Miller, J. R. Buck, A. Kuzmich, and H. J. Kimble, *Science* **303**, 1992 (2004).
 [14] M. Keller, B. Lange, K. Hayasaka, W. Lange, and H. Walther, *Nature (London)* **431**, 1075 (2004).
 [15] T. Legero, T. Wilk, M. Hennrich, G. Rempe, and A. Kuhn, *Phys. Rev. Lett.* **93**, 070503 (2004).

- [16] H. J. Carmichael, *An Open Systems Approach to Quantum Optics*, Lecture Notes in Physics m18 (Springer-Verlag, Berlin, 1993).
- [17] M. J. Hartmann, F. G. S. L. Brandao, and M. B. Plenio, *Nat. Phys.* **2**, 849 (2006).
- [18] T. Pellizzari, *Phys. Rev. Lett.* **79**, 5242 (1997).
- [19] A. Biswas and D. A. Lidar, *Phys. Rev. A* **74**, 062303 (2006).
- [20] Q. A. Turchette, C. J. Myatt, B. E. King, C. A. Sackett, D. Kielpinski, W. M. Itano, C. Monroe, and D. J. Wineland, *Phys. Rev. A* **62**, 053807 (2000).
- [21] C. J. Myatt, B. E. King, Q. A. Turchette, C. A. Sackett, D. Kielpinski, W. M. Itano, C. Monroe, and D. J. Wineland, *Nature (London)* **403**, 269 (2000).
- [22] S. Maniscalco, J. Piilo, F. Intravaia, F. Petruccione, and A. Messina, *Phys. Rev. A* **69**, 052101 (2004).
- [23] N. Stefanou and A. Modinos, *Phys. Rev. B* **57**, 12127 (1998).
- [24] M. Bayindir, B. Temelkuran, and E. Ozbay, *Phys. Rev. Lett.* **84**, 2140 (2000).
- [25] Y. Xu, Y. Li, R. K. Lee, and A. Yariv, *Phys. Rev. E* **62**, 7389 (2000).
- [26] L.-L. Lin, Z.-Y. Li, and B. Lin, *Phys. Rev. B* **72**, 165330 (2005).
- [27] S. Longhi, *Phys. Rev. A* **74**, 063826 (2006).
- [28] W. Yao, R.-B. Liu, and L. J. Sham, *Phys. Rev. Lett.* **95**, 030504 (2005).
- [29] M. D. Lukin, S. F. Yelin, and M. Fleischhauer, *Phys. Rev. Lett.* **84**, 4232 (2000).
- [30] M. Fleischhauer, S. F. Yelin, and M. D. Lukin, *Opt. Commun.* **179**, 395 (2000).
- [31] J. Dille, P. Nisbet-Jones, B. W. Shore, and A. Kuhn, *Phys. Rev. A* **85**, 023834 (2012).
- [32] F.-Y. Hong and S.-J. Xiong, *Phys. Rev. A* **76**, 052302 (2007).
- [33] J. Piilo, S. Maniscalco, K. Härkönen, and K.-A. Suominen, *Phys. Rev. Lett.* **100**, 180402 (2008).
- [34] J. Piilo, K. Härkönen, S. Maniscalco, and K.-A. Suominen, *Phys. Rev. A* **79**, 062112 (2009).
- [35] S. Maniscalco and F. Petruccione, *Phys. Rev. A* **73**, 012111 (2006).
- [36] B. Bellomo, R. Lo Franco, and G. Compagno, *Phys. Rev. Lett.* **99**, 160502 (2007).
- [37] C. W. Gardiner and P. Zoller, *Quantum Noise* (Springer-Verlag, Berlin, Germany, 2000).
- [38] M. O. Scully and M. S. Zubairy, *Quantum Optics* (Cambridge University Press, Cambridge, UK, 1997).
- [39] D. F. Walls and G. J. Milburn, *Quantum Optics* (Springer-Verlag, Berlin, 1994).
- [40] M. A. Nielsen and I. L. Chuang, *Quantum Computation and Quantum Information* (Cambridge University Press, Cambridge, UK, 2000).
- [41] C. H. Bennett and D. P. DiVincenzo, *Nature (London)* **404**, 247 (2000).
- [42] J. Zhang, Y.-X. Liu, R.-B. Wu, K. Jacobs, and F. Nori, *Phys. Rev. A* **87**, 032117 (2013).
- [43] C. W. Gardiner and M. J. Collett, *Phys. Rev. A* **31**, 3761 (1985).
- [44] G. S. Vasilev, D. Ljunggren, and A. Kuhn, *New J. Phys.* **12**, 063024 (2010).
- [45] P. Haikka and S. Maniscalco, *Phys. Rev. A* **81**, 052103 (2010).
- [46] H.-P. Breuer and F. Petruccione, *The Theory of Open Quantum Systems* (Oxford University Press, Oxford, UK, 2002).
- [47] H.-N. Xiong, W.-M. Zhang, M.-Y. Tu, and D. Braun, *Phys. Rev. A* **86**, 032107 (2012).
- [48] M. W. Jack, M. J. Collett, and D. F. Walls, *Phys. Rev. A* **59**, 2306 (1999).
- [49] T. Yu, L. Diósi, N. Gisin, and W. T. Strunz, *Phys. Rev. A* **60**, 91 (1999).
- [50] C. Cohen-Tannoudji and S. Reynaud, *J. Phys. B* **10**, 2311 (1977).